Journal of Energy Storage 77 (2024) 109827

Contents lists available at ScienceDirect

Journal of Energy Storage

journal homepage: www.elsevier.com/locate/est

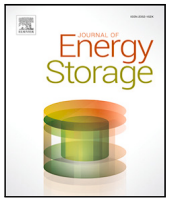

Research papers

Profitability of battery storage in hybrid hydropower–solar photovoltaic plants

Jonathan Fagerström [a,*], Soumya Das [a], Øyvind Sommer Klyve [a], Ville Olkkonen [b], Erik Stensrud Marstein [a]

[a] Department of Solar Power Systems, Institute for Energy Technology, Instituttveien 18, Kjeller, 2007, Viken, Norway
[b] Department of Energy Systems Analysis, Institute for Energy Technology, Instituttveien 18, Kjeller, 2007, Viken, Norway

ARTICLE INFO

Keywords:
Battery
Floating-PV
Hybrid power plant
Hydropower
PV
Techno-economic modeling

ABSTRACT

Increased energy demand and rapid environmental changes triggered by global greenhouse gas emissions have forced numerous countries to consider renewable energy sources (RES) as possible alternatives to conventional fossil-fuel energy sources. Due to the inherent uncertainty, intermittency, and generally uncontrollable power generation by single-source renewable power plants, hybrid power plants (HPPs) incorporating several mutually complementary RES have lately gained much interest. Integrating battery storage systems with such HPPs has the potential to run them more similarly to conventional fossil-fueled power plants, providing controllable power generation, and reducing its variability. Given such a future scenario and the lack of existing detailed studies, this paper investigates the profitability potential for a viable business case for battery storage integration with utility-scale hybrid hydropower–solar photovoltaic (PV) plants. The study presented here is based on a hypothetical, two-reservoir cascaded hydropower plant in Sub-Saharan Africa. The role of the battery is assessed by considering the overall profitability of the HPP when participating in capacity markets, ancillary services, and energy arbitrage. The relationship between the value stacking of battery services and its impact on battery life has been critically examined. This study provides estimates on increased profitability, cost-optimal battery capacities, battery degradation estimates, and the HPP-battery interoperability aspects under various hydropower and electricity market operating scenarios. Batteries will likely increase cost-effectiveness by co-optimization with PV-system as well as power market contracts. In this case, adding a battery increased the profitability by about 2% when combining revenues from capacity markets and ancillary services.

1. Introduction

Over the past decade, major economies of the world have increasingly focused on the utilization of renewable energy sources (RES) to fulfill their ever-rising energy demand. This has also been particularly necessary owing to climate change, the recent global energy crisis, and the sharp rise in electricity prices [1]. However, with more integration of RES into the existing grid system, uncertainty over power supply security has become a concern. Hybrid power plants (HPPs) provide a way forward in such a context by incorporating mutually complementary RES and suitable energy storage systems which substantially reduce power generation uncertainty. In addition, integrating battery storage systems into a RES-based hybrid power plant could increase the overall profitability by reducing energy losses, increasing the average value of the energy sold, and usually receiving incentives through tax credit [2].

Hydropower has historically been a significant source of renewable energy. In addition to providing clean energy, the added benefits of the hydropower plants are to provide a sustained water supply from the associated water reservoirs for irrigation and drinking, even during dry seasons. HPPs consisting of hydropower and floating photovoltaics (FPVs) have gained considerable interest in both research and industry [3–5]. The primary arguments for such hybrid plants are typically resource complementarity and better transmission equipment utilization that minimize costs [6]. For example, during the summer months when there are usually low water levels in the reservoirs resulting in lower hydropower production, PV power generation is high due to high solar irradiance. Conversely, during the winter while hydropower generation is high due to higher water levels in the reservoirs, PV power generation is low due to low solar irradiance [7]. This results in a more stable power output throughout the year for a hybrid hydro-FPV power plant. Conflicts arising from significant land usage by large

* Corresponding author.
E-mail address: Jonathan.Fagerstrom@ife.no (J. Fagerström).

https://doi.org/10.1016/j.est.2023.109827
Received 22 August 2023; Received in revised form 10 November 2023; Accepted 20 November 2023
Available online 1 December 2023

Index of Abbreviations and Notations:

Most of the important abbreviations and notations used in this study are provided here for quick reference. The others are described suitably in the remaining part of the text for ease of reading.

Abbreviations

PV	Photovoltaic
RES	Renewable energy sources
HPP	Hybrid power plants
FPV	Floating photovoltaic
GW	Gigawatt
LP	Linear programming
Li	Lithium
SoC	State of charge of a battery
USD	United States dollar
MUSD	Million USD
kWh	Kilowatt-hours
SEI	Solid electrolyte interface
DoD	Depth of discharge
PPA	Power purchase agreement
MW	Megawatts
MWp	Megawatts peak
ACp	Alternating current peak
HT	Hydro turbine
SoH	State of health of the battery
IQR	Interquartile range
chrg	Battery charging
dischrg	Battery discharging
Str	Battery stress

Notations

Z	Total cost involved
(i)	Index for the investment period
(o)	Index for the operating period
(IC_i)	Investment cost for the period (i)
(OC_i)	Operating cost for the period (i)
(x_i)	Investment variables for the period (i)
(y_{io})	Operational variables for the period (i) and (o)
(ζ_i)	Discount factor for the period (i)
(λ)	Discount rate
(σ)	Years in between each investment period
(γ)	Discount factor for the operating costs
(AC_i)	Cost of an asset for the period (i)
(M)	Asset lifetime
(C_{wavg})	Weighted average cost of capital
(CAP_{EXi})	Annual capital expenditure of the asset
(OP_{EXi})	Annual operational expenditure of the asset
(η)	Efficiency of the respective equipment
(ρ)	Density of water
(g)	Gravitational constant
(b)	Index for the battery
(w^{stor})	Energy stored in the battery
(v_b^{storEN})	Battery storage capacity (energy)
(v_b^{storPW})	Battery storage capacity (power)
(L)	Life of the battery
(deg)	Battery degradation

ground-based renewable energy projects [8], and consequent rises in the project costs [9] may also be mitigated by using FPVs that utilize the unused spaces on the reservoir surface of the hydropower plants. It has also been shown in some existing studies that enhanced cooling effects of the water bodies and reduced water evaporation may result in a higher heat loss coefficient [10] and better performance of FPVs compared to their ground-based counterparts [11]. However, the studies conducted by the authors in [12,13] show that FPVs only sometimes experience substantial water cooling, and the effect is extremely dependent on the system topology/technology and location. Nonetheless, hybrid hydro-FPV power plants have a great potential for development as only 25% coverage of the reservoir surfaces worldwide with FPVs shall result in 4400 GW of power [14].

Although there are many advantages to RES-based HPPs with battery storage, only a few studies have analyzed the role of batteries in hydro-PV plants. Nonetheless, as early as 2012, the efficacy of the battery and pumped hydro storage in hydro-PV plants was evaluated using a failure index, i.e. the number of times the power supply was not met [15]. In [16], the authors modeled a pumped storage hydropower plant and conducted a stability analysis of the plant integrated with a hybrid power system consisting of solar and wind power. Another research conducted a techno-economic analysis of an off-grid PV/wind/hydro system in Canada and concluded that pumped hydro was more cost-effective than batteries [17]. The authors in [18] analyzed the role of batteries for day-ahead scheduling of utility-scale hydro-wind-PV plants. Here, three objective functions were employed: minimization of operational risk, minimization of residual load deviation, and maximization of power delivery. Although cost-effectiveness was not determined, it was demonstrated that batteries could reduce operational risk, improve peak shaving performance, and boost daily power delivery. On a larger scale, the integration of battery and pumped hydro storage in the future Greek power system was studied, and it was determined that the combination of both short-term battery storage and long-term pumped hydro storage was cost-optimal [19]. A similar investigation for the Indian case [20] determined that batteries were not cost-effective when "round-the-clock" tender compliance was being designed.

The sizes of batteries for various markets and production technologies were evaluated in several studies, despite a lack of specific hydro-FPV-battery cases. The author in [21] conducted a qualitative and quantitative analysis of the value of energy storage in electricity generation and determined that storage in utility-scale plants could provide the following services: energy arbitrage, peaking capacity, transmission and distribution benefits, contingency reserves, load following, regulation reserve, frequency response, and black start. These eight services could be further categorized into three fundamental groups: energy arbitrage, capacity market, and ancillary services. It was determined that, among these services, ancillary services were the most valuable. The same three service categories were presented in a review of existing PV-battery hybrids in the United States [22]. In general, value stacking by participating in the wholesale market, that is, hybrid plants operating in merchant mode and engaging in energy arbitrage was found to be not the most profitable business model. Private business models centered on capacity markets (such as peak-load reductions and resiliency premiums) were more profitable but did not necessarily align with grid quality indicators. Value-stacking battery operations were found to increase battery profitability. However, to accomplish this, the battery must be designed to serve multiple markets, such as energy arbitrage, capacity markets, and ancillary services. A grid-connected British case demonstrated that value-stacking was required for profitability [23]. The authors also emphasized the significance of

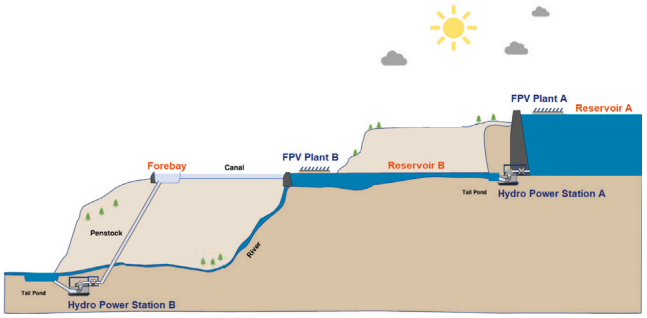

Fig. 1. System sketch of hybrid hydro-FPV-battery power plant.
Source: Modified from an image by Norconsult

evaluating the compatibility between various value-stacking services. This necessitates the consideration of diverse power/energy ratio requirements, as energy arbitrage can be designed for several hours, whereas some ancillary services only require a few minutes, often with a minimum power requirement. The timing of services must also be considered in terms of synergy to avoid situations in which two or more markets must be satisfied simultaneously.

It is observed from the literature review that over the last decade there has been much interest in the operation of hybrid hydro-FPV plants. A growing interest could also be observed in the recent mapping of methodologies and business models for battery storage in utility-scale power plants. However, to the best of the authors' knowledge, despite the battery energy storages having great potential for business cases in utility-scale hybrid hydro-FPV plants, none of the existing publications have analyzed such a scenario. The research study conducted here aims to bridge this knowledge gap. Therefore, the purpose of this study is to determine the potential for batteries to improve the cost-effectiveness of a hydro-FPV hybrid power plant. This is accomplished by examining a case in Sub-Saharan Africa and focusing on base load functionality and the relationship between the value stacking of battery services and battery aging. A mathematical optimization model based on multi-period linear programming (LP) formulation is used that simultaneously provides the cost-optimal FPV and battery capacities as well as the cost-optimal hydropower and battery system scheduling for each operating hour in a year.

1.1. Paper structure

The paper is organized as follows: Section 1 introduces the reader to the background of this study, reviews the existing research literature, provides the novelty and motivation for this study, and presents the paper's structural overview. Details of the hybrid power plant studied in this paper are provided in Section 2. Section 3 presents the results by comparing a base case (hydro-FPV) to a battery case (hydro-FPV-battery). The battery case results are subdivided into five subsections covering (1) profitability based on capacity market participation, (2) battery degradation, (3) value stacking capacity market with ancillary service, (4) profitability with energy arbitrage, and (5) a section on how the results are impacted by uncertain input data. Finally, Section 4 provides the concluding remarks.

2. Materials and methods

2.1. Optimization model

In this work, the role of battery energy storage systems in hybrid hydro-FPV power plants is evaluated based on a hypothetical hydropower plant in Sub-Saharan Africa, where the climatic conditions fall within the As zone of the Køppen climate classification. The hydropower plant consists of two cascaded reservoirs and two hydro turbines, with the proposed FPV installation on the reservoir surfaces, as depicted in Fig. 1. Since this work assumes that FPV and battery systems are added to an existing hydropower plant, both hydropower and power grid capacities were fixed and restricted to 126 MW. The mathematical optimization model based on multi-period linear programming (LP) formulation simultaneously provides the cost-optimal FPV and battery capacities as well as the cost-optimal hydropower and battery system scheduling for each operating hour in a year. Hence, the operation strategy of the hybrid power plant is a result of the cost-optimization model. The two flexible assets, hydro turbines and battery, operate according to the schedule that results in the lowest yearly total cost. The model is implemented in the JuMP framework [24] with Julia programming language [25] and is thoroughly described in [26]. The authors would like to refer the reader to [26] for the details of the optimization model. However, the abstract formulation of the optimization problem is presented in Eqs. (1)–(4). The objective here is to minimize the annual discounted system capital and operational expenditures of the hybrid power plant and maximize the revenues from selling electricity to the market. This can be formulated as a combined minimization problem:

$$\min_{x,y} Z = \sum_{i \in I} \zeta_i \left(IC_i x_i + \gamma \sum_{o \in O} \left(OP_i - p_{io} \right) y_{io} \right) \tag{1}$$

Here, Z represents the total cost comprising of investment cost IC_i and operating cost OP_i. $i \in I$, where I is the total number of investment periods and $o \in O$, where O is the total number of operational periods. ζ_i converts all future costs to the first investment period, with an annual discount rate of λ during σ years in between each investment period. It is defined as follows:

$$\zeta_i = (1+\lambda)^{-\sigma(i-1)} \tag{1a}$$

Similarly, γ is defined as:

$$\gamma = \sum_{o=0}^{\sigma-1} (1+\lambda)^{-o} \tag{1b}$$

The solution of the optimization problem provides the user with the investment variables in terms of generation, storage, and grid capacity. Thus, considering the asset's lifetime as M during the model horizon $|P|$ $(p \in P)$, IC_i is given as:

$$IC_i = \frac{1-(1+\lambda)^{-min(\sigma|P|-p+1,\ M)}}{1-\frac{1}{1+\lambda}} AC_i \tag{1c}$$

$$AC_i = \frac{C_{wavg}}{1+C_{wavg}-\left(1+C_{wavg}\right)^{1-M}} CAP_{EX\,i} + OP_{EX\,i} \tag{1d}$$

Here, $OP_{EX\,i}$ is assumed to be fixed.

The constraints for the objective function (1) are as follows:

$$\alpha_i x_i \le \beta_i \tag{2}$$

$$y_{io} - \phi_{ih} x_i \le D_{io} \tag{3}$$

$$x_i, y_{io} \ge 0 \tag{4}$$

Constraint (2) is an inequality constraint that ensures that the lifetime of the asset is considered across the investment periods. Constraint (3) ensures that the operation of the asset is bounded by the investment decision, its availability, and for balancing the demand D_{io}. ϕ_{io} provides the availability of the asset for the investment period i and operational period o. Lastly, constraint (4) ensures non-negative values of the investment variables.

It is to be noted here that in this paper, the optimization is carried out for a single investment period of 1 year, but the mathematical model is formulated as a generalized tool to handle multi-period optimization as per the user requirement.

Table 1
Hydropower plant parameters.

Parameter	Unit	System A	System B
Turbine power	MW	36	90
Reservoir capacity	Mm^3	1169	12
Flow min	Mm^3/h	0	0.11
Flow max	Mm^3/h	0.58	0.72
Average head	m	20.5	50

2.2. Hydropower modeling

In this paper, the characteristics of the hydropower plants are considered constant throughout the simulation period and are described in Table 1. This work also assumes a constant efficiency of 90% for the hydro turbines and generators combined. In addition, a constant head level, which is the average of the maximum and minimum head levels is assumed for each of the respective reservoirs. Thus, the power production from turbine j in plant k is:

$$y_o^k = \sum_j \left(d_{oj}^k \bar{\eta}_j^k \left(\bar{h}_o^k - h_{tail}^k - h_{loss}^k \right) \right) \rho g \tag{5}$$

Here, d_{oj}^k is the water discharge from the jth turbine in kth plant at the oth operating period. Similarly, $\bar{\eta}_j^k$ is the corresponding turbine efficiency, $\bar{h}_o^k$ is the average water head level, h_{tail}^k is the tail head level and h_{loss}^k is the lost head level.

It should be noted that the efficiency of the turbine and generator, which is treated as constant in our model, theoretically varies with discharge and head levels. The constant efficiency has been chosen to correspond to the average efficiency over a typical Francis turbine and generator set's common discharge ranges, but this simplification will alter the optimal hydro discharge schedule. However, the overall energy output from the hydropower plant is presumed to be only marginally affected by this approximation, thus negligibly affecting the valuation of the battery storage. Implementing this simplification significantly reduces the simulation runtime.

Three historical hydro inflow years on monthly resolution are used to model the hydropower resource availability for a median, dry and wet year. Since the hydropower plant is designed to operate in Sub-Saharan Africa with prevailing tropical to arid climatic conditions, evaporative water loss from its reservoirs plays a vital role in the overall operation of the plant. Substantial amounts of water are lost due to evaporation, especially during the dry years, affecting power production. To account for this effect, the product of the reservoir areas during operation and the corresponding monthly evaporation rate (available for one weather year) is deducted from the water inflow in the median, dry, and wet weather years. Consequently, the simulation obtains much more realistic results than situations where water evaporation is not considered. Regarding reservoir level restrictions, the model dictates that the water levels in the reservoir at the end of the simulation match those at the beginning.

2.3. FPV modeling

To select the cost-optimal FPV capacity, capacity factors for the median, dry, and wet hydro inflow years are modeled with PVGIS-SARAH2 irradiance data on hourly resolution using the Photovoltaic Geographical Information System (PVGIS) tool version 5.2 [27] The modeled FPV system is assumed to be south oriented, with a 13 degree fixed tilt, consisting Cryst-Si PV modules having 19.9% module efficiency, and with total system losses of 13%. The cost-optimal FPV inverter size (dc-ac ratio) and corresponding clipping losses are selected when solving the optimization model. It is also assumed that the FPV installation reduces water evaporation from the reservoir area it covers by 60% [28]. The water balance equation is formulated to capture the changes in reservoir volume and water flow between the hydropower plants. Water evaporation from the reservoir surfaces is modeled in a similar way as described in [26]. Key assumptions and the important parameters for the FPV are stated in Table 2.

Table 2
Floating PV parameters, partly adopted from [29].

Parameter	Unit	Value
FPV		
Capital cost	USD/kWp	1220
Operational cost	USD/kWp/year	15.5
Lifetime	years	25
Module efficiency	%	19.9
Panel tilt	degrees	13
System losses	%	13
Inverter		
Capital cost	USD/kW	40
Lifetime	years	15

Table 3
Battery system parameters.

Parameter	Unit	Value
Capital cost	USD/kWh	326
Operational cost	USD/kWh/year	0.35
Lifetime	years	15
Round-trip efficiency	%	85
Available SoC	%	80
Maximum cycles	–	4500
C-rate	–	1

2.4. Battery modeling

In this paper, the proposed hybrid hydro-FPV-battery power plant is assumed to employ Li-ion LFP battery components. The initial input conditions for the battery unit are shown in Table 3. Using the model's energy balance, the battery component monitors the state of charge (SoC) and energy throughput to meet the boundary conditions. The battery storage balance Eq. (6) is set as a difference between the storage content in the previous hour minus the net discharge taking into account the charging/discharging efficiency ($\eta_b^{chrg/dischrg}$),

$$w_{o-1,b}^{stor} + \eta_b^{chrg} y_{ob}^{chrg} - \frac{y_{ob}^{dischrg}}{\eta_b^{dischrg}} = w_{ob}^{stor} \tag{6}$$

$$SOC_{b,min} v_b^{storEN} \leq w_{ob}^{stor} \leq SOC_{b,max} v_b^{storEN} \tag{7}$$

$$0 \leq y_{ob}^{chrg/dischrg} \leq v_b^{storPW} \tag{8}$$

In (7), the storage content (w_{ob}^{stor}) is constrained by the minimum and maximum SOC levels, which are defined as percentage of the battery storage capacity (energy). In (8) the battery charging/discharging power rate, $y_{ob}^{chrg/dischrg}$ is constrained between zero and the battery storage capacity (power). The energy output is used to calculate the maximum number of full equivalent charging–discharging cycles (henceforth described as cycles), which is considered as 4500. In addition, the model stipulates that the SoC at the end of the modeling period must equal the SoC at the beginning of the period. It is assumed that the battery has a SoC level of 50% at the beginning of the simulation period. The input conditions are shown in Table 3 and were adopted from [30,31]. These input data will undoubtedly influence the net present cost calculations, so, sensitivity analyses were conducted to show how capital cost, round-trip efficiency, maximum cycles, and C-rate influence profitability.

Even though a battery lifetime of 15 years is a reasonable estimate, an additional degradation model was used to validate this assumption and determine if the specific charging and discharging cycles of the modeled case would have a significant impact on the battery's lifetime. The deployed model can be found at [32] and was based on the work of [33]. The battery degradation was modeled using two models: a linear and a non-linear model. The nonlinear model is defined

by a combination of two exponential decay processes according to Eqs. (9)–(10).

$$L = 1 - \alpha_{\text{sei}}\, e^{-t\beta_{\text{sei}}\deg_t} - (1 - \alpha_{\text{sei}})\, e^{-t\deg_t} \tag{9}$$

$$L = 1 - \alpha_{\text{sei}}\, e^{-N\beta_{\text{sei}}\deg_c} - (1 - \alpha_{\text{sei}})\, e^{-N\deg_c} \tag{10}$$

L denotes the life of the battery and therefore equals 0 for a new battery, α_{sei} and β_{sei} are parameters of the solid electrolyte interface (SEI) model, t is the time period, N is the number of cycles, deg_t represents the battery degradation per time period and deg_c is the battery degradation per cycle.

N in Eq. (10) is determined using a rainflow cycle counter, that processes the input data set containing SOC data, and calculates the DOD and average SOC of each unique cycle, as well as the number of occurrences of such cycles in the SOC dataset. This data is subsequently utilized together with the other stress models to calculate cycle degradation. Differentiating between the magnitude DOD and average SOC is important since the cycles can have various paths and might also remain at specific SOC levels for some time before the cycle is considered completed.

The linear degradation model calculates both the calendar and cycling degradation of the battery based on different stress models. Calendar degradation (11) is calculated based on time, average state of charge, and temperature. Cycling degradation (12) is calculated for each battery cycle by factoring in the stress due to depth of discharge (DoD), SoC, and temperature.

$$deg_t = Time_{Str} \times SoC_{Str} \times Temp_{Str} \tag{11}$$

$$deg_c = DoD_{Str} \times SoC_{Str} \times Temp_{Str} \tag{12}$$

These stresses are multiplied for each cycle to determine the cumulative cycling degradation. In this context, DoD_{Str} represents the degradation caused by how much of the battery's capacity has been used in each cycle, SoC_{Str} represents the effect of the battery's charge level, and temperature stress represents the impact of high operating temperatures on the battery. The different stress models are illustrated in (13)–(16).

$$Time_{Str} = k_t t \tag{13}$$

$$SoC_{Str} = e^{k_{SoC}(SoC - SoC_{ref})} \tag{14}$$

$$Temp_{Str} = e^{k_T(T - T_{ref})} \tag{15}$$

$$DoD_{Str} = k_{d1}\, DoD\, e^{k_{d2} DoD} \tag{16}$$

The coefficients used in the specific stress models: k_t, k_{soc}, k_T, k_{d1}, and k_{d2} are extracted from experimental data by separating each stress factor. As an example, k_t is determined by comparing degradation at a reference temperature with the degradation from another temperature point. The variables T_{ref} and SoC_{ref} are reference values and are used to designate significant conditions or levels within the model. The variables t, T, SoC, and DoD represent time, temperature, state of charge condition, and discharge depth, respectively. In summary, experimental data for parameter fitting were obtained from the study [32], and battery SoC-data from simulations were utilized to estimate the degradation according to the different stress models. Table 4 summarizes the model parameters used in this work.

The rationale for having the degradation model split into calendar and cycling, as well as the choice for having the specific stress models covering SoC, DoD, time, and temperature, is explained in [33].

Table 4
Model parameters for battery degradation model.

α_{sei}	β_{sei}	k_t	k_{soc}	SoC_{ref}
5.75E−2	1.21E2	4.11E−10	1.01	0.5
k_T	T_{ref}	k_{d1}	k_{d2}	
6.71E−2	25	9.05E−6	1.40	

2.5. Cost assumptions

The FPV-system's techno-economic parameters are displayed in Table 2, [34]. Similar battery parameters are displayed in the Table 3. Using data from [30,31], the total system cost for a battery with C-rate 1 in the year 2030 was calculated. Additionally, sensitivity analyses were conducted to determine the effect of lower/higher capital costs on profitability.

It is presumed that the hybrid power plant participates in a power purchase agreement (PPA) setting. In terms of price, technology, shape, and duration, PPA formulations vary significantly. In this study, a two-level configuration is assumed to represent a scenario in which electricity is more valuable during daytime. In this scenario, the high price level (100 USD/MWh) is in effect for 12 h, from 06:00 to 18:00, whereas the low-price level (60 USD/MWh) is in effect for the remaining hours. The same two-level shape persists throughout the entire year. The structure in terms of firm peak and off-peak hours for the hypothetical PPA scheme was provided by a local renewable power producer. The tariff price levels were estimated based on the average spot prices during the peak and off-peak hours using the historical spot price data from 2014 to 2021. Due to lack of data availability for the location of the case study, the used data is based on historical Southern African Power Pool (SAPP) spot price market data [35]. The optimization model calculates the fixed power levels, i.e., how many megawatts (MW) are to be produced within the two respective price levels, and excess power is sold on the wholesale market at 50 USD/MWh, which is slightly less than the low PPA level to encourage this hybrid plant to function as a base load plant. The purchase of electricity from the grid to cover the PPA commitments was prohibited.

3. Results and discussions

3.1. Base case

This paper's base case consists of one 36 MW (hydro turbine A: HT_A) and one 90 MW (hydro turbine B: HT_B) hydro turbine, as well as a 143 MWp floating PV with a 105.3 MW converter. The FPV capacity for the base case is determined through cost-optimization considering no battery storage and initial PPA schedule. It is described later in more detail in Section 3.2. As stated earlier, the grid capacity is based on the total rated hydro capacity which is 126 MW, and the hybrid power plant with FPV results in an excess installed power generation capacity of 84%, which helps in the better utilization of the grid [6]. The water reservoir inflows and FPV production are depicted in Fig. 2 and exhibit a pronounced dry and rainy season seasonal pattern. However, FPV production is consistent throughout the year.

With the assumed resource inflows and techno-economic assumptions, the cost-optimal PPA power levels were 12.7 MW (PPA2 at 60 USD/MWh) and 118.6 MW (PPA1 at 100 USD/MWh), as depicted in Fig. 3 alongside the FPV production profile for the first day in April in the dry season. A similar production profile for the first day of November, which corresponds to the wet season is shown in Fig. 4.

The water flow through HT_B was restricted to 0.11 M m^3/h and the load factor was consequently kept over 14%, while HT_A was allowed to be shut down. The hydropower turbines were simulated

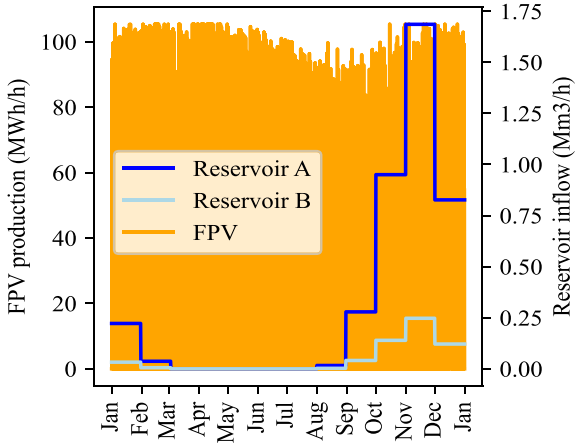

Fig. 2. Annual correlation between FPV production and hydro reservoir inflow.

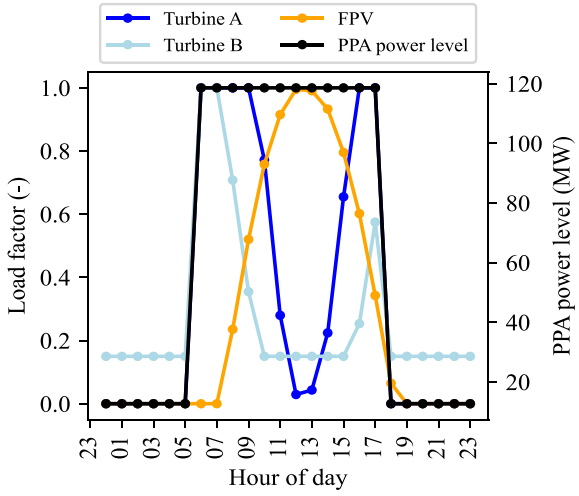

Fig. 3. Load factor for generators and PPA power levels for one day in the dry season (1 April).

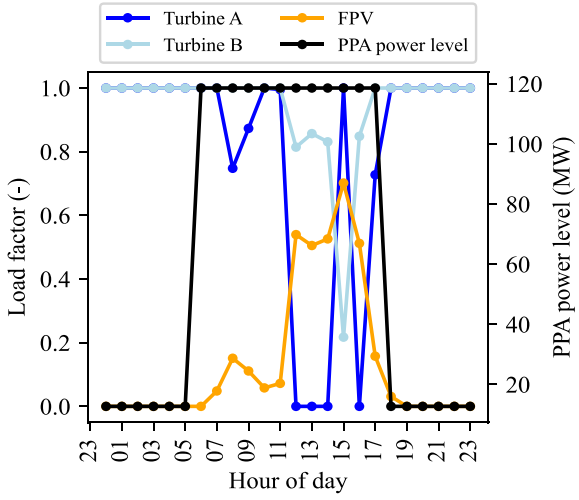

Fig. 4. Load factor for generators and PPA power levels for one day in the wet season (1 November).

with constant efficiency and without restrictions on ramping rates. With these assumptions, Fig. 3-Fig. 4 show the load factor of the three generators during the two different seasons, and Table 5 shows the monthly average load factor for the turbines.

Table 5
Monthly average load factor of generators.

Month	Turbine A	Turbine B	FPV
1	0.32	0.31	0.28
2	0.36	0.29	0.28
3	0.38	0.31	0.25
4	0.35	0.28	0.29
5	0.36	0.29	0.28
6	0.39	0.31	0.25
7	0.40	0.32	0.24
8	0.42	0.34	0.22
9	0.49	0.45	0.20
10	0.68	0.91	0.21
11	0.68	0.89	0.23
12	0.86	0.85	0.23

Table 6
System design and profitability with different PPA structures. Annual profit increase is compared against the base case.

PPA1 schedule	Battery (MWh)	FPV (ACp)	PPA1 (MW)	PPA2 (MW)	Annual profit increase (%)
06–18	0.0	105.3	118.6	12.7	0.0
06–19	10.1	116.8	116.0	10.0	0.7
06–20	64.3	131.2	118.6	7.1	0.6
06–21	32.5	123.4	103.5	9.8	−0.5
05–18	28.3	117.6	117.9	7.6	−1.6

Table 7
Power production volumes and shares for the different markets.

Power market market	Annual production (MWh/year)		Fraction of total production (%)	
	Base	Battery	Base	Battery
PPA1	519 303	605 854	73.4	80.3
PPA2	55 802	26 514	7.9	3.5
Wholesale	132 296	121 780	18.7	16.1

3.2. Battery case

3.2.1. Profitability in capacity market

For the sake of simplicity and grouping of revenue streams, here capacity markets are used to describe an extension of PPA contracts since this enables the power plant to ensure power generation capacity outside of normal operating hours. The profitability of battery systems was initially determined by analyzing additional revenue creation in a capacity market setting by calculating the net present cost for different PPA configurations. Table 6 illustrates how extending the duration of the PPA1 schedule affects cost-optimal battery capacity. The 14-hour duration (06:00–20:00) yielded the greatest battery capacity, whereas the 13-hour duration (06:00–19:00) yielded the greatest profitability relative to the base case. Additionally, shifting the PPA1 duration to the evening was more profitable than extending the morning hours.

The design for 06:00–20:00 PPA is referred to as the "Battery case". The generated energy volumes for the different markets are presented in Table 7, and show that volumes in PPA1 increased to greater than 80.3% while PPA2 decreased to 3.5%. Wholesale energy volumes were 4.6 times higher than the PPA2 energy volumes, despite the wholesale prices being lower than PPA2 prices. The Battery case allowed for a 25% larger FPV system and the PV-share to total production increased from 32.0% to 36.7%. HT_B still remained the major power generator, as shown in Table 8.

Since the results in Table 6 were based on a co-optimization of FPV and battery, it is unclear whether the annual profit increase is a

Table 8
Power production volumes and shares by technology.

Technology Technology	Annual production (MWh/year)		Fraction of total production (%)	
	Base	Battery	Base	Battery
FPV	226 227	277 102	32.0	36.7
HT_A	139 635	149 819	19.7	19.9
HT_B	344 030	333 743	48.6	44.3

Table 9
Comparison of system and PPA power level design and annual profit increase for different optimization constraints. Annual profit increase is compared against the base case.

Case	Specifics	Battery (MWh)	FPV (MWp)	DC/AC ratio	PPA1 (MW)	PPA2 (MW)	Annual profit increase (%)
Hydro + FPV	Base case	0.0	143.0	1.36	118.6	12.7	–
Hydro + FPV + Battery	Optimizing both FPV & battery sizes	64.3	184.0	1.40	118.6	7.1	**0.6%**
Hydro + FPV	Fixed FPV size as in the optimized case	0.0	184.0	1.40	107.8	10.8	−1.3%
Hydro + FPV + Battery	Base-case FPV size & optimized battery size	64.3	143.0	1.36	107.0	7.1	−1.7%

result of increased power production from the FPV plant or flexibility provided by the battery system. Two additional simulations were therefore conducted to determine the annual profit increase for other power plant configurations, and the results are presented in Table 9. The co-optimized case, in which both battery and FPV are optimized for cost-efficiency, increases profitability by 0.6% compared to the base case. When the FPV was constrained to the same dimensions as in the co-optimized configuration (184 MWp) and the battery was omitted, the profit decreased by 1.3%; consequently, this case is not cost-effective. When the FPV was limited to the same size as the base case (143 MWp), and the battery was limited to the same size as the co-optimized case (64.3 MW), cost-effectiveness declined by 1.7%. This suggests that the incorporation of a battery improves the cost-effectiveness of the hybrid plant by supporting the implementation of a larger FPV plant. The value of co-optimization of PV-battery systems has been discussed previously [36] and was shown here to produce a more favorable PPA with an increase in PPA1 production. Thus, the incorporation of a battery into hybrid hydro-FPV power plants facilitates the creation of more lucrative contracts for the capacity market.

3.2.2. Battery degradation

Since the optimization model did not account for battery degradation, an additional lifetime assessment was conducted using a separate degradation model. The SoC profiles of the battery cases have been run through the degradation model to determine how different input power conditions affect the assumption of a 15-year life expectancy. Fig. 5 displays the Battery case results from Table 6 and indicates that the assumption is plausible if temperatures are kept under control. The remaining capacity after 15 years at a temperature of 25 °Celsius is about 83%. It is generally accepted that batteries are defined to have reached their End-of-Life when their state of health reaches 80% [37], still in some cases, they can continue to operate if performance and safety conditions are sufficient.

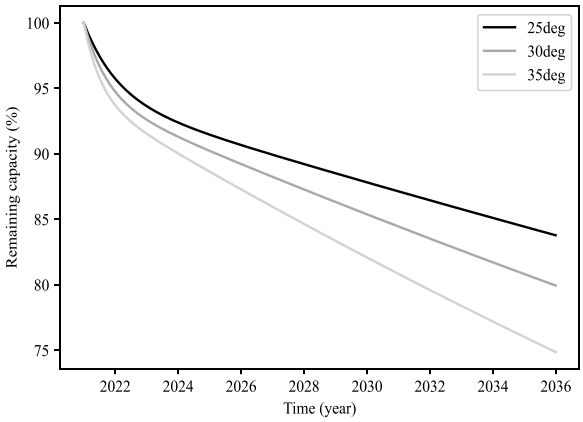

Fig. 5. Remaining capacity in the battery at different temperatures for the case with fixed power price.

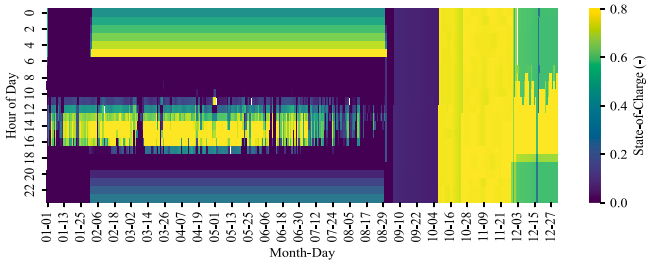

Fig. 6. Battery state-of-charge for the full year presented as hourly values in a heat map.

3.2.3. Value stacking with ancillary service market

The potential for value stacking was assessed by analyzing patterns in battery operation. Fig. 6 shows an overview of the state-of-charge for the entire year and displays that the battery is cycled less during the autumn. By comparing the battery SoC, as depicted in Fig. 6, with the inflow of hydro resources, as illustrated in Fig. 2, it becomes evident that the battery undergoes significant cycling during the dry period, whereas its activity is comparatively reduced during the wet period. The high hydro inflow during the autumn is sufficient to both uphold PPA power levels without the need for a battery and still fill reservoirs before the year-end, which is a condition to be met in the optimization model. Based on Fig. 6 it seems reasonable to assume that the battery could be made available for ancillary services for 3–4 months (September to November/December) when hydro inflows are high.

During the dry season, the battery is used twice daily, both during the first and last hour of the high PPA. Charging occurs both during the day with excess PV production and during the evening and night at low PPA prices. The battery is therefore unavailable for other services from 05:00 to 21:00, as PPA1 is active from 06:00 to 20:00 and requires 1 h of charging before and after its operation. Based on the hybrid plant's schedule, it seems reasonable to assume that the battery could be made available for ancillary services during dry season nights (21:00–05:00) and full days during September–November/December. More details around the battery discharging events can be seen in Fig. A.20.

As there is no market for ancillary services in the Sub-Saharan Africa, market conditions from other regions were used to estimate how value-stacking could enhance the profitability of batteries in this specific case. One such example is the DS3-market in Ireland [38], where the authors estimated revenues for a 1 MW battery to be about 319 000 €/year, or 36 €/MW/h. The specific ancillary service products used to generate revenue in [38] originated from Fast Frequency Reserves as well as Primary, Secondary, and Tertiary Reserves, which all adhere to

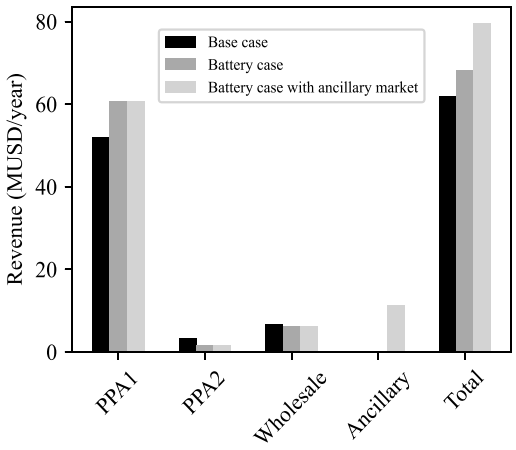

Fig. 7. Annual revenue generated by three configurations of hybrid power plants. The base case is compared to the battery case with and without ancillary service revenues.

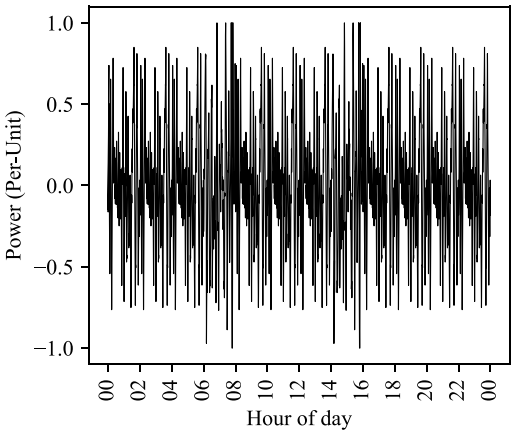

Fig. 8. Frequency regulation signal expressed as the per-unit value during 24 h.

Table 10
Number of cycles and their respective DoD during a full day of frequency regulation for the battery case.

DoD (%)	Cycles (–)
1.5	145
3.0	44
4.5	19
6.0	12
7.5	0
9.0	10
10.5	1
12.0	2

a frequency drop curve and are designed to provide power in time intervals ranging from seconds to twenty minutes. Using the same hourly rate (36 €/MW/h) but reducing the available hours as per the previous discussion, the battery in our case would generate approximately 11 MUSD annually. This assumption also requires the grid connection capacity to accommodate full power supply from the battery system, hence the hydro turbines cannot operate at nominal power. Fig. 7 shows the revenue streams and demonstrates that ancillary services could potentially contribute significantly to the total annual revenue of the power producer. The cost of ancillary services is 48% greater than the sum of PPA2 and the wholesale market. In comparison to the base case, the battery case with ancillary services generates nearly 18 MUSD more in total revenue. Although the conditions for the Irish ancillary service market do not necessarily comply with the Sub-Saharan market, this calculation shows the principles behind determining the potential for value stacking

But since the battery state of health (SoH) is assumed to reach approximately 83% after 15 years of operation in the PPA setting and 80% is generally regarded as the replacement threshold, there is little space for additional cycling before the battery must be replaced. Since the degradation estimation in Fig. 5 only incorporates cycling according to the PPA schedule and does not account for additional wear from frequency regulation, a supplementary analysis was necessary. This is accomplished using frequency regulation data [39]. The per-unit signal of the data is depicted in Fig. 8 and the corresponding battery SoC is depicted in Fig. 9. The data set has a duration of 24 h, and the per-unit value changes every four seconds. As shown in Table 10, a full day of frequency regulations required 233 cycles with 12% DoD as the highest value, but a vast majority of cycles at 1.5% DoD. Since the battery is required to be scheduled for PPA service the majority of the time, frequency regulation can only be scheduled for 8 h, from 21:00 to 05:00, to allow for one hour of battery charging before and after frequency regulation. Hence, it is assumed that the simultaneous provision of ancillary services and discharge in capacity markets is not feasible, an assumption that seems to be true for the majority of markets. In the scenario where a battery is generating nominal power to the capacity market, the battery cannot provide power during an event for frequency response. One could argue that occurrences of this nature are infrequent, and the potential revenue generated from battery systems could potentially offset any penalties incurred as a result of failing to meet contractual power obligations. This study did not take into account such possibilities. Table 11 displays the number of cycles with each DoD for the reduced hours, which totals 84 cycles with approximately 8% DoD. This would add approximately 31,000 cycles per year, or 460,000 cycles over 15 years. According to Fig. 10, a DoD of 10% results in a cycle lifetime of 198,000 cycles. Consequently, value stacking frequency regulation with PPA operations would have a significant impact on the assumed battery longevity in this instance. As the battery input data indicated 198,000 cycles (10% DoD) until 80% SoH, this implies that an additional 29,700 cycles are conceivable before reaching 80% SoH. 29,700 cycles are 6% of 460,000, which means that a value stacking capacity market (PPA-generation) with an ancillary market would increase annual revenue by 660,000 USD (6% of 11 MUSD) for 15 years. Adding this revenue to the total annual cost in Table 6 improves the annual profit increase from 0.6% to 2.0%. Despite being a somewhat synthetic and overarching calculation, this example showcases both the potential profitability increase from ancillary services as well as the challenges with value stacking and battery wear from excessive cycling.

The potential for value stacking in this instance is therefore not only dependent on the duration and timing of events, i.e. when during the day and year the battery is available for providing supplementary services, but also on the battery degradation from additional cycling. Since the cost optimization model's objective function did not account for revenues from ancillary services, it was not feasible to optimize the battery based on revenues from both ancillary services and capacity markets. It is possible that the cost-optimal battery size would increase if both value streams were included, given that a larger battery capacity would also extend the battery's lifetime, thereby allowing for more cycling and revenue generation. For a more detailed understanding of the wear from value stacking services with such distinctly different cycling characteristics, it would be useful to conduct battery aging experiments at small DoD windows at various SoC levels, given that the majority of cycles occur within a few percent of DoD.

3.2.4. Profitability of energy arbitrage

Energy arbitrage is usually defined as the market for electricity trading, i.e. the purchase and sale of electricity based on spot price

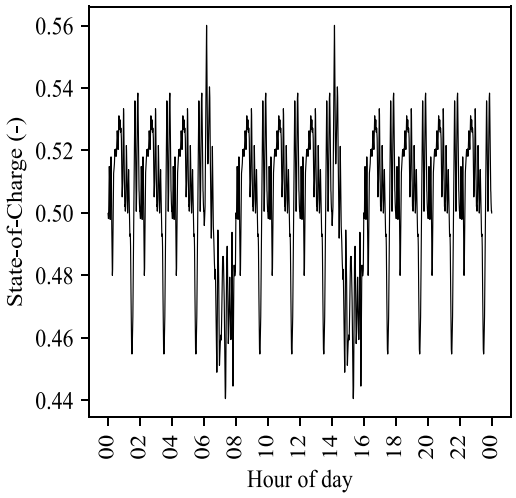

Fig. 9. Battery state-of-charge during charging/discharging according to the frequency signal.

Table 11
Number of cycles, timing of cycles, and their respective DoD during value stacking with capacity market for battery case.

DoD (%)	Cycles (–) Hour 21-24	Cycles (–) Hour 00-05
1.0	17	32
2.1	4	8
3.1	3	5
4.2	3	3
5.2	0	0
6.3	1	3
7.4	1	0
8.4	2	2

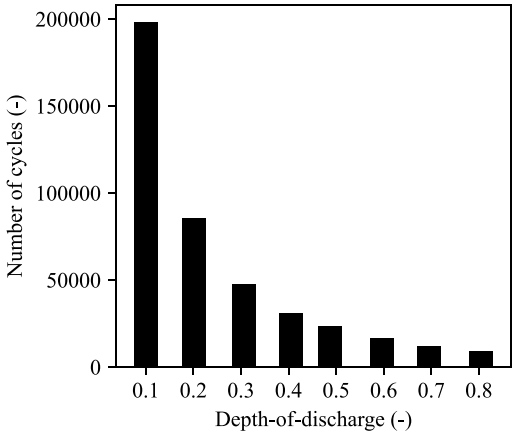

Fig. 10. Cycle lifetime as function of depth-of-discharge for LFP battery.

signals. The wholesale market has a significant impact on the design of power plants, and spot prices are likely the most uncertain input data in these analyses. In this work, the profitability of energy arbitrage market participation was analyzed by including a variable spot price at three different price levels. Figs. 11–13 depicts the spot price statistics that illustrate the monthly temporal fluctuations. The difference between the low and high spot prices is not only linked with the average values, but also with the monthly spread, as the high price show a greater number of outliers. These figures do not, however, account for the dynamics of price fluctuations within shorter time intervals, such as within a single day, which are typically important to energy arbitrage.

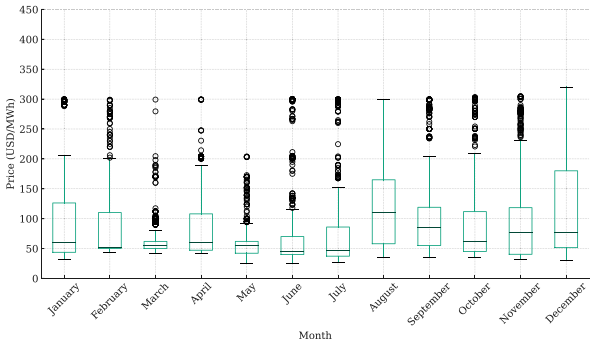

Fig. 11. Boxplot showing wholesale market prices representing the high spot price. The boxes show the interquartile range (IQR), the median is the horizontal line within each box, the whiskers are 1.5 times IQR, and the outliers are denoted by dots.

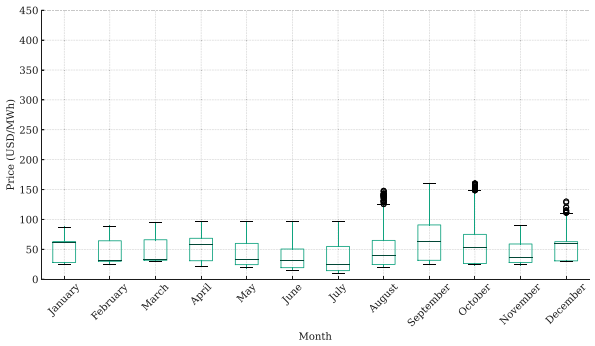

Fig. 12. Boxplot showing wholesale market prices representing the low spot price. The boxes show the interquartile range (IQR), the median is the horizontal line within each box, the whiskers are 1.5 times IQR, and the outliers are denoted by dots.

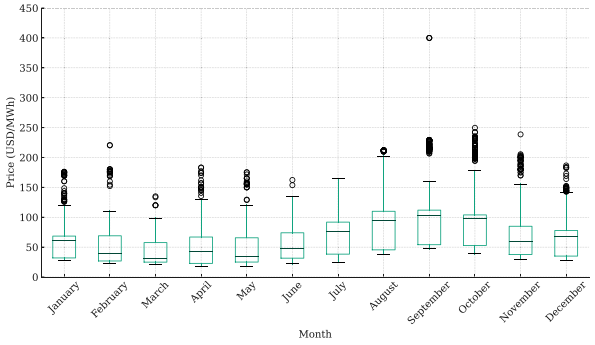

Fig. 13. Boxplot showing wholesale market prices representing the median spot price. The boxes show the interquartile range (IQR), the median is the horizontal line within each box, the whiskers are 1.5 times IQR, and the outliers are denoted by dots.

Unless otherwise specified, the purchase of electricity was not allowed, implying that the potential increased profitability from this market is gained from a redistribution of production volumes in PPA1, PPA2, and wholesale markets.

The outcomes of the power plant and PPA design for various spot prices are presented in Table 12, which demonstrates that batteries are not profitable at low and median wholesale prices. In the scenario with high wholesale prices, a smaller battery is optimal from a cost perspective, but the PV capacity to be installed is significantly reduced and is likely included for battery charging. If the battery and FPV capacities are fixed to 64.3 MWh and 184.0 MWp, as in the battery case with the fixed price, and median spot prices are used, profitability is marginally increased, but the likelihood of stacking with ancillary services decreases due to heavy cycling. More details on the frequency

Table 12
Power plant and PPA design for different wholesale market scenarios. Annual profit increase compared against the battery case with fixed price. A positive value denotes an increase in profitability.

Wholesale market	Annual average price (USD/MWh)	Battery capacity (MWh)	FPV DC (MWp)	DC/AC ratio	PPA1 (MW)	PPA2 (MW)	Annual profit increase (%)
Fixed price	50	64.3	184.0	1.40	118.6	7.1	
Spot Low	49	0.0	155.3	1.37	104.4	12.7	−1.9%
Spot Median	66	0.0	138.1	1.37	94.4	12.7	4.1%
Spot High	94	29.7	50.2	1.35	0.0	0.0	45.3%
Spot Median *	66	64.3	184.0	1.40	112.7	8.6	2.2%

* battery and FPV sizes are fixed in simulation.

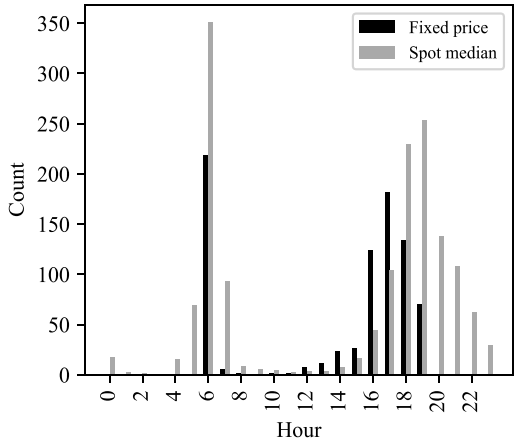

Fig. 14. Comparison of annual battery discharging events for a case with fixed wholesale market price (50 USD/MWh) and median spot price (66 USD/MWh).

of battery discharging events is shown in Fig. A.19. During the months of October to December, the battery is cycled both at night and in the evening, reducing the time available for participation in providing ancillary services. Fig. 14 summarizes the two cases' annual discharge events. Note that due to the unavailability of a wholesale market in Sub-Saharan Africa, the current prices used here are examples from specific years on the wholesale market in South Africa [35]. Nevertheless, the results here indicate that value stacking of battery operations for more valuable PPA design and ancillary services is a more stable long-term solution than energy arbitrage on the wholesale market. However, if the power market matures to include dynamic spot prices, it is probable that batteries will continue to be profitable based on this data set. This aspect should however be analyzed in more detail. In order to reach a broader understanding of the general profitability of batteries in hybrid hydro-PV power plants, more studies focusing on revenue generation in mature power markets would be valuable.

Battery degradations for the three different wholesale market prices were assessed with the degradation model and did not indicate any major differences. This can also be seen in Table 13 where the cycle counts for the three cases are presented.

3.2.5. Sensitivity analyses

Impact of resource inflow on system design: The water resource inflows vary from year to year, and Table 14 illustrates how the hybrid plant would be designed for dry and rainy year conditions. In both extreme instances, batteries are cost-effective, but battery capacity and PPA levels vary. The median year produced the greatest PV-battery systems and the most aggressive PPA contracts. Furthermore, we investigated how PPA levels could be maintained with the use of batteries assuming that the hybrid plant is designed based on median-year conditions. Table 15 presents results for dry-year conditions and indicates that a battery of 241.6 MWh and an FPV-system of 264.6 MWp would be required if power purchases are prohibited. Moreover, if purchased

Table 13
Number of cycles at different DoD during the 15-year lifetime for different wholesale market prices compared to number of cycles in battery specifications. Fixed price denotes the Battery case; Median and High prices imply hourly spot prices at the median and high price levels.

DoD (%)	Cycles (–) Fixed price	Cycles (–) Median price	Cycles (–) High price	Cycles (–) Battery specs
10	2295	2880	5100	198 000
20	270	255	405	85 100
30	601	151	256	47 200
40	210	91	181	30 900
50	121	135	675	23 200
60	105	150	180	16 300
70	285	2250	60	12 000
80	5430	4020	5340	8 870

Table 14
System and PPA power level design and annual profit increase for extreme resource inflow conditions. Annual profit increase is compared against the median year.

	Battery (MWh)	FPV (MWp)	DC/AC ratio	PPA1 (MW)	PPA2 (MW)	Annual profit increase (%)
Dry	2.9	164.3	1.44	82.4	12.7	−35%
Median	64.3	183.9	1.40	118.6	7.1	
Wet	20.2	156.9	1.36	115.0	11.0	11%

Table 15
System design for dry-year conditions and varying electricity purchase prices. PPA levels were maintained at 118.6 and 7.1 MW, and annual profit increased relative to the median resource inflow. Positive values indicate profitability growth.

Electricity cost (USD/MWh)	Battery (MWh)	FPV DC (MWp)	DC/AC ratio	Grid purchase (MWh)	Annual profit increase (%)
190	241.6	264.6	1.52	0.0	−39%
170	218.4	250.6	1.51	11 118	−39%
150	169.4	225.8	1.47	34 220	−38%
130	36.0	197.6	1.57	89 892	−35%
110	0.0	182.9	1.61	111 503	−31%
110 *	64.3	183.9	1.40	91 361	−32%

* Battery and FPV sizes are fixed in simulation.

electricity was used to offset the production shortfall, the results indicate that it would be more profitable to purchase electricity from the grid than invest in a battery. To withhold the PPA levels for the Battery case (64 MWh battery), the facility would need to purchase 91 361 MWh or approximately one-third of the FPV production. Similarly, Table 16 presents results for wet-year conditions and demonstrates that PV-battery systems can be significantly smaller to meet the PPA levels without power purchases from the grid and that if power purchases are permitted, smaller quantities are required to compensate for production deficits.

Overall, this demonstrates that withholding PPA levels during dry-year conditions necessitates the modification of PPA contracts, compensation through power purchases, or the installation of larger battery systems. Compensation through the procurement of electricity was more cost-effective.

Impact of PPA price spread: Both the annual price and the difference between the highest and lowest PPA prices may vary based on factors such as the type of power production technology, geographic location, duration of the contract, the volume of purchased energy, market conditions, and creditworthiness [40]. To determine how the price spread of such time-of-use PPAs affects the profitability of batteries, sensitivity analyses are conducted according to Table 17. In these instances, the annual average price is approximately 83 USD/MW, which falls within the range specified by [40]. It is, however, marginally higher than the

Table 16
System design for wet-year conditions and varying electricity purchase prices. PPA levels were maintained at 118.6 and 7.1 MW, and annual profit increased relative to the median resource inflow. Positive values indicate profitability growth.

Electricity cost (USD/MWh)	Battery (MWh)	FPV DC (MWp)	DC/AC ratio	Grid purchase (MWh)	Annual profit increase (%)
210	32.5	166.9	1.36	0	11%
190	31.1	166.5	1.36	414	11%
170	10.0	161.4	1.37	7417	11%
150	0.2	161.0	1.42	10 163	11%
130	0.0	159.5	1.41	11 175	12%
110	0.0	151.8	1.36	16 596	12%
110 *	64.3	183.9	1.40	0	8%

* Battery and FPV sizes are fixed in simulation.

Table 17
Impact of PPA price split on power plant design and profitability. Annual profit increase compared against Battery case. Positive numbers denote increase in profitability.

PPA1/PPA2 prices (USD/MWh)	Battery capacity (MWh)	FPV DC (MWp)	DC/AC ratio	PPA1 (MW)	PPA2 (MW)	Annual profit increase (%)
105/55	88.2	191.6	1.40	122.7	3.3	6.2%
104/56	87.9	191.7	1.40	122.7	3.3	4.9%
103/57	71.1	185.4	1.40	119.6	6.4	3.7%
102/58	68.3	184.8	1.40	119.2	6.8	2.4%
101/59	64.7	183.9	1.40	118.6	7.1	1.2%
100/60	64.3	183.9	1.40	118.6	7.1	
99/61	50.0	177.2	1.39	115.4	8.6	−1.2%
98/62	18.5	164.7	1.38	108.8	12.0	−2.3%
97/63	11.0	159.5	1.38	106.9	12.3	−3.4%
96/64	3.3	155.9	1.38	105.1	12.7	−4.4%
95/65	0.0	152.9	1.38	104.2	12.7	−5.4%

price used in an India study [20], where the base case was 70 €/MW (≈ (75 USD/MW), and sensitivity analyses ranged from 30–130 €/MW. As predicted, the profitability and optimal battery size increase with the spread, as shown in Table 17. At a spread of 30 USD/MWh, the battery system becomes unprofitable when used exclusively for PPA operations.

Impact of battery parameters: The simulations used a battery cost of 326 USD/kWh, and Fig. 15 illustrates how both higher and lower costs affect the cost-optimal battery capacity. The high cost (500 USD/kWh) is comparable to the cost of batteries today, and batteries are not cost-effective at these prices without additional value stacking. At lower prices though, installed battery capacity doubles and the annual profit increases by about 2%–5%. Although a bit hypothetical, its interesting to see that while the annual profit increases from 2% at 200 USD/MWh to 5% at 100 USD/MWh, the cost-optimal capacity remains fairly stable.

Fig. 16 illustrates the relationship between battery system efficiency and battery capacity, demonstrating a dramatic decrease in capacity when system efficiency declines to lower than 85%. In this investigation, 85% was utilized, which appears achievable in battery systems if the temperature is controlled [41] and power flows are kept greater than 10% of nominal power to avoid converter losses [42]. While the cost-optimal battery capacity wont increase much at higher system efficiencies than 85%, the annual profit increases by 0.2–0.3% if higher system efficiencies are achieved.

The impact of battery cycle lifetime on profitability was also analyzed by testing five different cycle lifetimes (7500, 6000, 4500, 3000, 1500). It was found that 4500 cycles are required for profitability, whereas 3000 cycles or less are insufficient. A certain number of cycles are thus required to fulfill the PPA requirements for the entire year.

Another sensitivity parameter that was evaluated was the C-rate. Five C-rates were evaluated (2, 1, 0.5, 0.25, and 0.1), and it was found

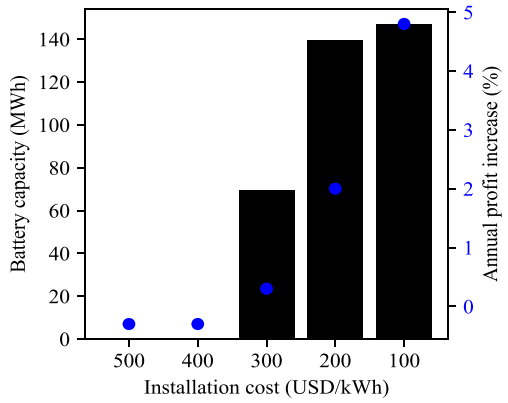

Fig. 15. Cost-optimal battery capacity and annual profit increase at different battery installation costs. The installation cost represents batteries with C-rate 1 and the profit increase is relative to the battery base case with an installation cost of 326 USD/kWh.

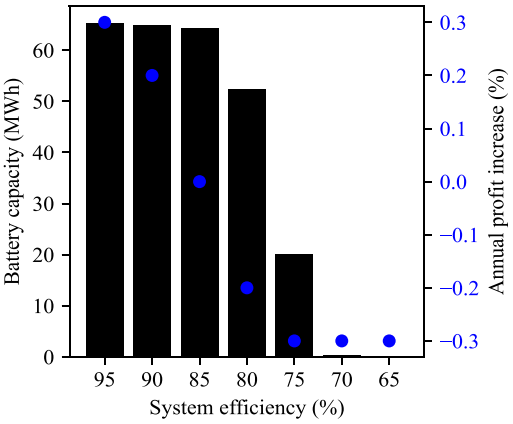

Fig. 16. Cost-optimal battery capacity and annual profit increase at different battery system efficiency levels. The profit increase is relative to the battery base case with a system efficiency of 85%.

that only a C-rate of 1 was profitable. In comparison to other studies, this C-rate is relatively high. A study of utility-scale PV-battery systems determined that for energy systems with PV shares lower than 12.5%, a C-rate of 0.5 was the most cost-effective, whereas a C-rate of 0.17 was the most cost-efficient for energy systems with PV shares over 25% [43]. The same study also found that the cost-optimal battery power rating was 25% of PV capacity. Following these numbers, our system would be cost-optimal with 46 MW battery converter and 276 MWh battery storage capacity. However, higher C-rates pair well with value stacking with ancillary services that typically prioritize power over capacity, as demonstrated in [44], where it was found that a C-rate value of 3.5 was the most cost-effective. Since it sounds somewhat confusing to find the "optimal" C-rate, future work on battery system design should include more details on C-rate. It might even be reasonable to investigate hybrid battery systems, where one energy battery (low C-rate) and one power battery (high C-rate) are connected to one converter. This could reduce total installation cost and increase efficiency and lifetime since specific flexibility demands of the power plant can be served by two different batteries. Besides more in-depth quantifications of possible cost-savings, there is additionally a need for testing the more sophisticated integration between energy management system of the converter and the two battery management systems.

4. Conclusion

This paper has analyzed the profitability of battery systems in hybrid hydro-PV power plants in the context of a conceptual hybrid

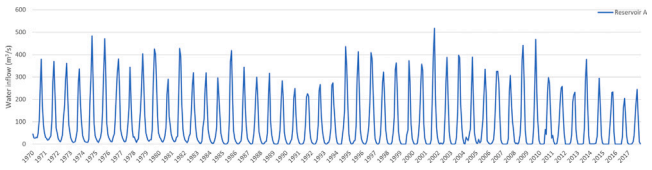

Fig. A.17. Historical water inflow rate of Reservoir A.

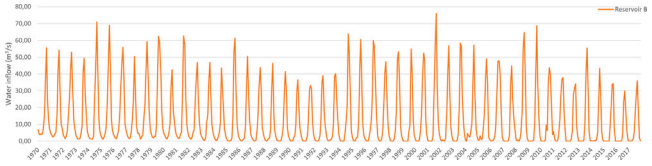

Fig. A.18. Historical water inflow rate of Reservoir B.

hydro-FPV power plant by determining the revenue generated from capacity markets, ancillary services, and energy arbitrage. A case study in Sub-Saharan Africa was utilized and the power plant functionality was geared towards base load functionality. Emphasis was placed on value stacking of battery functions for improved revenue generation, but excessive battery wear and life expectancy were also considered.

The intention of this paper was thus to answer the general question "Are batteries profitable for hydro-PV plants?", using a specific case study. This obviously implies that certain assumptions are necessary and that it is impossible to cover every aspect of power plant economics. However, based on the findings, the following conclusions are highlighted:

- The addition of batteries increased the cost-effectiveness of the power plant by 0.6% at a battery cost of 330 USD/kWh when operating solely in capacity markets.
- Value stacking capacity markets with ancillary services further improved the cost-effectiveness and made the power plant 2.0% more cost-effective than the base case without batteries.
- Battery cycle lifetime restricted full value stacking of capacity market and ancillary services.
- The power plant was more cost-efficient with batteries because of co-optimization benefits, i.e. the battery enabled installation of higher PV capacities in addition to increased flexibility resources.
- Energy arbitrage provided economic benefits for the hydro-FPV power plant, but batteries were not necessary, and variable spot prices make predictability and value stacking difficult.

The findings of this work are relevant to hybrid plants situated in regions where capacity markets dominate over wholesale markets and where the power plant is connected to the grid via a single point of connection. In these settings, carefully considering a battery system will likely have a positive impact on cost-efficiency by co-optimization of the PV-capacity as well as contracts related to PPAs and ancillary service markets. To achieve a higher degree of generality regarding battery profitability in hybrid hydro-PV plants, future work is encouraged to focus on hybrid plants situated in wholesale markets, where PPA contracts are non-existing and the plant operates in a multi-market setting where scheduled power generation should be coordinated with ancillary service markets, all through the constraints set by the single point of connection to the power grid. A more sophisticated hydropower model should also be developed to incorporate the reservoir volume and head relationship, as well as the dynamic turbine and generator efficiency dependencies. With these model features, it would be feasible to assess how a battery system might enhance cost-effectiveness by maintaining the hydropower turbines at a more efficient operational set-point.

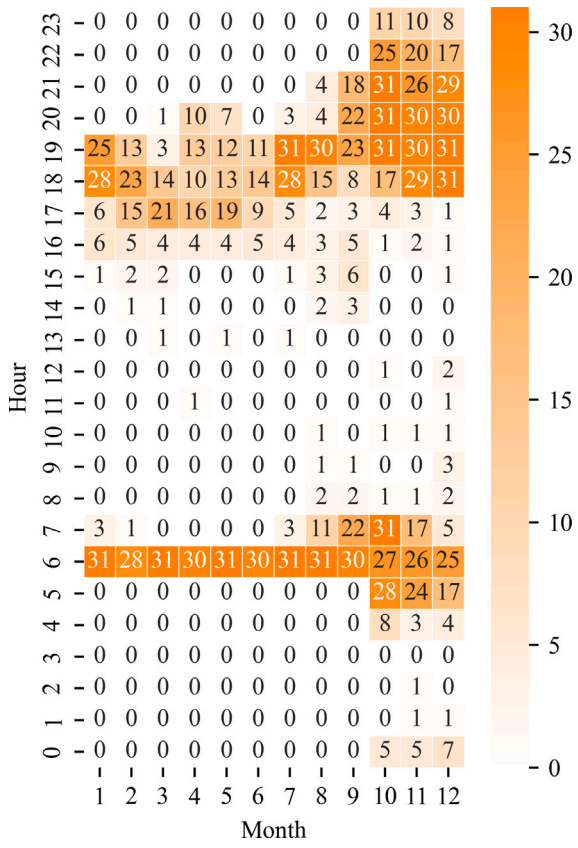

Fig. A.19. Number of monthly discharge events each hour for the case with variable median spot price.

Funding

This research was funded by the Research Council of Norway (RCN), Norway, project number 328640 and the APC was funded by RCN, Norway.

CRediT authorship contribution statement

Jonathan Fagerström: Conceptualization, Methodology, Formal analysis, Writing – original draft. **Soumya Das:** Writing – original draft, Writing – review & editing, Supervision. **Øyvind Sommer Klyve:** Validation, Investigation. **Ville Olkkonen:** Software. **Erik Stensrud Marstein:** Supervision, Project administration, Funding acquisition.

Declaration of competing interest

The authors declare the following financial interests/personal relationships which may be considered as potential competing interests: Jonathan Fagerstrom reports financial support was provided by Research Council of Norway. Soumya Das reports financial support was provided by Research Council of Norway. Oyvind Sommer Klyve reports financial support was provided by Research Council of Norway. Ville Olkkonen reports financial support was provided by Research Council of Norway. Erik Stensrud Marstein reports financial support was provided by Research Council of Norway.

Data availability

Data will be made available on request.

Acknowledgment

All authors have read and agreed to the published version of the manuscript.

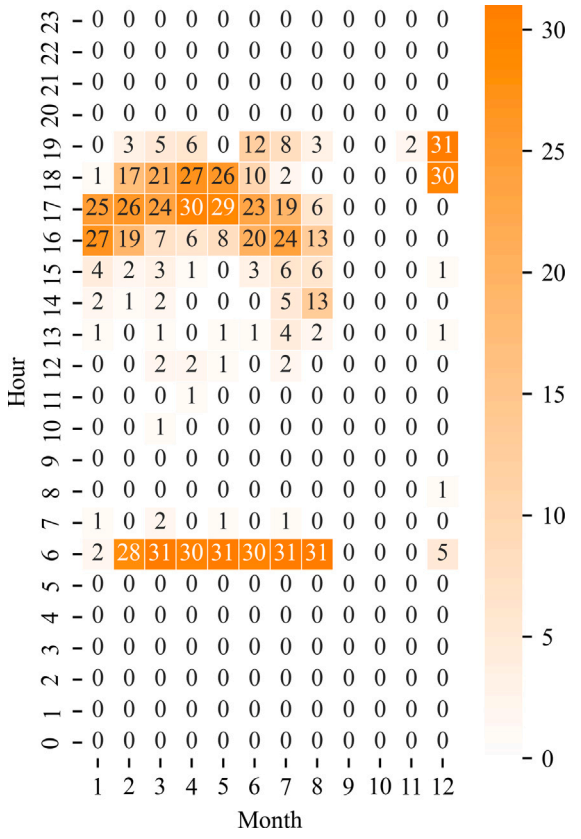

Fig. A.20. The number of monthly discharge events each hour during a full year for the Battery case operating in the capacity market.

Appendix. Historical water inflow rates of the reservoirs and monthly discharge events

Fig. A.17 and Fig. A.18 show historical water inflow to reservoirs from year 1970 to 2017. This raw data was used to construct the dry, wet, and median years used in the optimizations.

References

[1] International Energy Agency, Electricity Market Report, Technical Report, OECD, IEA, Paris, 2023, http://dx.doi.org/10.1787/f0aed4e6-en, URL: https://www.iea.org/reports/electricity-market-report-2023.

[2] W. Gorman, C.C. Montañés, A. Mills, J.H. Kim, D. Millstein, R. Wiser, Are coupled renewable-battery power plants more valuable than independently sited installations? Energy Econ. 107 (2022) http://dx.doi.org/10.1016/j.eneco.2022.105832.

[3] R. Gonzalez Sanchez, I. Kougias, M. Moner-Girona, F. Fahl, A. Jäger-Waldau, Assessment of floating solar photovoltaics potential in existing hydropower reservoirs in Africa, Renew. Energy 169 (2021) 687–699, http://dx.doi.org/10.1016/j.renene.2021.01.041.

[4] N. Lee, U. Grunwald, E. Rosenlieb, H. Mirletz, A. Aznar, R. Spencer, S. Cox, Hybrid floating solar photovoltaics-hydropower systems: Benefits and global assessment of technical potential, Renew. Energy 162 (2020) 1415–1427, http://dx.doi.org/10.1016/j.renene.2020.08.080.

[5] E. Bellini, The world's first large scale hybrid hydro-floating solar power plant, 2021, Pv Mag., URL: https://www.pv-magazine.com/2021/09/13/the-worlds-first-large-scale-hybrid-hydro-floating-solar-power-plant/.

[6] R. Cazzaniga, M. Rosa-Clot, P. Rosa-Clot, G.M. Tina, Integration of PV floating with hydroelectric power plants, Heliyon 5 (6) (2019) e01918, http://dx.doi.org/10.1016/j.heliyon.2019.e01918.

[7] H. Liu, V. Krishna, J. Lun Leung, T. Reindl, L. Zhao, Field experience and performance analysis of floating PV technologies in the tropics, Prog. Photovolt., Res. Appl. 26 (12) (2018) 957–967, http://dx.doi.org/10.1002/pip.3039.

[8] Y. kuang Chen, J.G. Kirkerud, T.F. Bolkesjø, Balancing GHG mitigation and land-use conflicts: Alternative Northern European energy system scenarios, Appl. Energy 310 (January) (2022) http://dx.doi.org/10.1016/j.apenergy.2022.118557.

[9] R. Chiabrando, E. Fabrizio, G. Garnero, The territorial and landscape impacts of photovoltaic systems: Definition of impacts and assessment of the glare risk, Renew. Sustain. Energy Rev. 13 (9) (2009) 2441–2451, http://dx.doi.org/10.1016/j.rser.2009.06.008.

[10] H. Nisar, A. Kashif Janjua, H. Hafeez, S. Shakir, N. Shahzad, A. Waqas, Thermal and electrical performance of solar floating PV system compared to on-ground PV system-an experimental investigation, Sol. Energy 241 (June) (2022) 231–247, http://dx.doi.org/10.1016/j.solener.2022.05.062.

[11] S. Oliveira-Pinto, J. Stokkermans, Assessment of the potential of different floating solar technologies – Overview and analysis of different case studies, Energy Convers. Manag. 211 (March) (2020) 112747, http://dx.doi.org/10.1016/j.enconman.2020.112747.

[12] D. Lindholm, T. Kjeldstad, J. Selj, E.S. Marstein, H.G. Fjær, Heat loss coefficients computed for floating PV modules, Prog. Photovolt., Res. Appl. 29 (12) (2021) 1262–1273, http://dx.doi.org/10.1002/pip.3451.

[13] A.F. Skomedal, M.B. Ogaard, H. Haug, E.S. Marstein, Robust and fast detection of small power losses in large-scale PV systems, IEEE J. Photovolt. 11 (3) (2021) 1–8, http://dx.doi.org/10.1109/JPHOTOV.2021.3060732.

[14] J. Farfan, C. Breyer, Combining floating solar photovoltaic power plants and hydropower reservoirs: A virtual battery of great global potential, Energy Procedia 155 (2018) 403–411, http://dx.doi.org/10.1016/j.egypro.2018.11.038.

[15] A. Beluco, P. Kroeff de Souza, A. Krenzinger, A method to evaluate the effect of complementarity in time between hydro and solar energy on the performance of hybrid hydro PV generating plants, Renew. Energy 45 (2012) 24–30, http://dx.doi.org/10.1016/j.renene.2012.01.096.

[16] B. Xu, D. Chen, M. Venkateshkumar, Y. Xiao, Y. Yue, Y. Xing, P. Li, Modeling a pumped storage hydropower integrated to a hybrid power system with solar-wind power and its stability analysis, Appl. Energy 248 (May) (2019) 446–462, http://dx.doi.org/10.1016/j.apenergy.2019.04.125.

[17] M.S. Islam, B.K. Das, P. Das, M.H. Rahaman, Techno-economic optimization of a zero emission energy system for a coastal community in Newfoundland, Canada, Energy 220 (2021) 119709, http://dx.doi.org/10.1016/j.energy.2020.119709.

[18] Y. Guo, B. Ming, Q. Huang, P. Liu, Y. Wang, W. Fang, W. Zhang, Evaluating effects of battery storage on day-ahead generation scheduling of large hydro–wind–photovoltaic complementary systems, Appl. Energy 324 (August) (2022) 119781, http://dx.doi.org/10.1016/j.apenergy.2022.119781.

[19] G.N. Psarros, S.A. Papathanassiou, Electricity storage requirements to support the transition towards high renewable penetration levels – Application to the Greek power system, J. Energy Storage 55 (PC) (2022) 105748, http://dx.doi.org/10.1016/j.est.2022.105748.

[20] E. Andreae, T.V. Jensen, D.E.M. Bondy, K. Heussen, Sizing hybrid power plants under round-the-clock tender compliance in India, in: 2022 Int. Conf. Renew. Energies Smart Technol., IEEE, 2023, pp. 1–6, http://dx.doi.org/10.1109/rest54687.2022.10022596.

[21] A.M. Elshurafa, The value of storage in electricity generation: A qualitative and quantitative review, J. Energy Storage 32 (June) (2020) 101872, http://dx.doi.org/10.1016/j.est.2020.101872.

[22] J. Seel, C. Warner, A. Mills, Influence of business models on PV-battery dispatch decisions and market value: A pilot study of operating plants, Adv. Appl. Energy 5 (December 2021) (2022) 100076, http://dx.doi.org/10.1016/j.adapen.2021.100076.

[23] S. Yamujala, A. Jain, R. Bhakar, J. Mathur, Multi-service based economic valuation of grid-connected battery energy storage systems, J. Energy Storage 52 (PA) (2022) 104657, http://dx.doi.org/10.1016/j.est.2022.104657.

[24] I. Dunning, J. Huchette, M. Lubin, JuMP: A modeling language for mathematical optimization, SIAM Rev. 59 (2) (2017) 295–320, http://dx.doi.org/10.1137/15M1020575.

[25] J. Bezanson, A. Edelman, S. Karpinski, V.B. Shah, Julia: A fresh approach to numerical computing, SIAM Rev. 59 (1) (2017) 65–98, http://dx.doi.org/10.1137/141000671.

[26] V. Olkkonen, K. Haaskjold, Ø.S. Klyve, R. Skartlien, Techno-economic feasibility of hybrid hydro-FPV systems in Sub-Saharan Africa under different market conditions, Renew. Energy 215 (2023) 118981, http://dx.doi.org/10.1016/j.renene.2023.118981.

[27] European Commission, PVGIS 5.2, 2022, EU Sci. Hub, URL: https://joint-research-centre.ec.europa.eu/pvgis-online-tool/pvgis-releases/pvgis-52_en.

[28] F. Bontempo Scavo, G.M. Tina, A. Gagliano, S. Nižetić, An assessment study of evaporation rate models on a water basin with floating photovoltaic plants, Int. J. Energy Res. 45 (1) (2021) 167–188, http://dx.doi.org/10.1002/er.5170.

[29] V. Ramasamy, D. Feldman, J. Desai, R. Margolis, U.S. solar photovoltaic system and energy storage cost benchmark: Q1 2021, Natl. Renew. Energy Lab. (September) (2021) 1–120, URL: https://www.nrel.gov/docs/fy21osti/77324.pdf.

[30] K. Mongird, V. Fotedar, V. Viswanathan, V. Koritarov, P. Balducci, B. Hadjerioua, J. Alam, Energy Storage Technology and Cost Characterization Report 2019, Technical Report, July, 2019, pp. 1–120, URL: https://energystorage.pnnl.gov/pdf/PNNL-28866.pdf.

[31] W. Cole, A.W. Frazier, W. Cole, A.W. Frazier, Cost Projections for Utility-Scale Battery Storage : 2020 Update, Nat. Renew. Energy Lab., Technical Report June, 2020, URL: https://www.nrel.gov/docs/fy21osti/79236.pdf.

[32] J.-Y. Morille, Predicting the degradation of a lithium-ion battery based on its operating profile, and operating conditions, 2017, URL: https://github.com/jymorille/lithium_ion_battery_degradation.

[33] B. Xu, A. Oudalov, A. Ulbig, G. Andersson, D.S. Kirschen, Modeling of lithium-ion battery degradation for cell life assessment, IEEE Trans. Smart Grid 9 (2) (2018) 1131–1140, http://dx.doi.org/10.1109/TSG.2016.2578950.

[34] D. Feldman, V. Ramasamy, R. Fu, A. Ramdas, J. Desai, R. Margolis, U.S. Solar Photovoltaic System and Energy Storage Cost Benchmark: Q1 2020, Natl. Renew. Energy Lab., Technical Report September, 2021, pp. 1–120, URL: https://www.nrel.gov/docs/fy21osti/77324.pdf.

[35] SAPP, The Southern African power pool, 2015, URL: https://www.sappmarket.com.

[36] J. Fagerström, K.A. Espegren, J. Selj, A. Severinsen, Forecasting and technoeconomic optimization of PV-battery systems for commercial buildings, Eceee Summer Study Proc. 2019-June (Simshauser 2016) (2019) 949–954.

[37] WG 6 Batteries Europe ETIP, Roadmap on Stationary Applications for Batteries, Technical Report, 2018, pp. 1–53, URL: https://energy.ec.europa.eu/system/files/2022-01/vol-6-009.pdf.

[38] M. Bahloul, M. Daoud, S.K. Khadem, A bottom-up approach for techno-economic analysis of battery energy storage system for Irish grid DS3 service provision, Energy 245 (2022) http://dx.doi.org/10.1016/j.energy.2022.123229.

[39] D.R. Conover, A.J. Crawford, J. Fuller, S.N. Gourisetti, V. Viswanathan, S.R. Ferreira, D.A. Schoenwald, D.M. Rosewater, Protocol for Uniformly Measuring and Expressing the Performance of Energy Storage Systems, Vol. PNNL-22010, Off. Electr. Deliv. Energy Reliab. Technical Report April, (April) 2016, pp. 1–101, URL: https://energystorage.pnnl.gov/pdf/PNNL-22010Rev2.pdf.

[40] L. Mendicino, D. Menniti, A. Pinnarelli, N. Sorrentino, Corporate power purchase agreement: Formulation of the related levelized cost of energy and its application to a real life case study, Appl. Energy 253 (July) (2019) 113577, http://dx.doi.org/10.1016/j.apenergy.2019.113577.

[41] Y. Deng, C. Feng, J. E, H. Zhu, J. Chen, M. Wen, H. Yin, Effects of different coolants and cooling strategies on the cooling performance of the power lithium ion battery system: A review, Appl. Therm. Eng. 142 (April) (2018) 10–29, http://dx.doi.org/10.1016/j.applthermaleng.2018.06.043.

[42] M. Schimpe, M. Naumann, N. Truong, H.C. Hesse, S. Santhanagopalan, A. Saxon, A. Jossen, Energy efficiency evaluation of a stationary lithium-ion battery container storage system via electro-thermal modeling and detailed component analysis, Appl. Energy 210 (November 2017) (2018) 211–229, http://dx.doi.org/10.1016/j.apenergy.2017.10.129.

[43] E. Virguez, X. Wang, D. Patiño-Echeverri, Utility-scale photovoltaics and storage: Decarbonizing and reducing greenhouse gases abatement costs, Appl. Energy 282 (October 2020) (2021) http://dx.doi.org/10.1016/j.apenergy.2020.116120.

[44] Y. Lin, B. Li, T.M. Moiser, L.M. Griffel, M.R. Mahalik, J. Kwon, S.M. Alam, Revenue prediction for integrated renewable energy and energy storage system using machine learning techniques, J. Energy Storage 50 (January) (2022) 104123, http://dx.doi.org/10.1016/j.est.2022.104123.